J Mater Sci (2007) 42:6769–6778
DOI 10.1007/s10853-006-1430-8

Wear behavior of TiB_2 inoculated 20Cr–3Mo–4C high chromium white cast irons

Serdar Osman Yilmaz

Received: 3 January 2006 / Accepted: 12 December 2006 / Published online: 26 April 2007

Abstract FeTi, B_2O_3, Al, and FeW particulates, approximately 40–60 μm in size, were mixed in stoichiometric ratio and sintered at 1,200 °C. The sintered particulates were added as 5 wt% to molten high chromium white cast iron over 50 C-deg above the melting temperature, and stirred at 1,000 rpm. The samples were investigated in three groups: (1) high Cr white cast iron inoculated by the particulates sintered from Al–FeTi–B_2O_3 particulates; (2) high Cr white cast iron inoculated by the sintered particulates derived from Al–FeTi, B_2O_3, and FeW particulates; and (3) specimens of the second group that were subsequently homogenized. The microhardness of ceramic particulates was measured as 2,800–3,400 HV_{10}. The effect of sintered particulate volume fraction on the abrasive wear resistance of the high chromium white cast iron was determined. The wear resistance and hardness of the composites improved significantly as a result of particulate inoculation. The application of the homogenization heat treatment to the inoculated samples produced a microstructure having homogeneously distributed particulates.

Introduction

Materials having high chromium concentration are used in a variety of applications including the mining and mineral processing, and cement production industries. These alloys have high abrasive wear resistance; hence, these alloys are used for applications where grinding, milling, and pumping apparatus are required to process hard materials such as ore, coal, gravel, and cement. The abrasive wear resistance of these materials is high due to hard carbides in the structure [1–4].

The alloys having high Cr contents have proeutectic and/or eutectic M_7C_3 carbides in a softer iron matrix. The matrix structure observed most often in the as-cast high Cr alloys is austenite. In addition, the carbides in the structure of these alloys are typically of the M_7C_3 type (M = Fe, Cr). The M_7C_3 carbides grow as rods and blades with their long axes parallel to the heat flow direction in the mold [5, 6].

Wear resistance is a function of chemical composition, processing conditions, and heat treatment; each alloy system must be evaluated with respect to these variables, as well as the tribological environment [7]. In the case of materials having high Cr, important microstructural parameters for wear resistance include the quantity, orientation, and morphology of carbides [8–14], the type of matrix [13, 14], and the interface between hard phase and the matrix [8, 9]. These factors also influence the hardness and fracture toughness of the material. The microstructure of white cast irons is similar to metal matrix composites (MMCs). There are two types of foundry methods for making composites with externally added particles, depending on the temperature at which the particles are introduced in the melt. In the liquid metallurgy process [15], the particles are added above the liquidus temperature of the molten alloy. In this processes, a vortex is used, and, for this reason, the composites have high porosity [16]. Several factors influence the final product, one very important being the metal melt's ability to wet the ceramic particles [17–20]. The wettability depends on many parameters: the type of particles, their shape, size, surface

S. O. Yilmaz (✉)
Department of Metallurgy, Faculty of Technical Education, University of Firat, Elazig 23119, Turkey
e-mail: osyilmaz@firat.edu.tr

roughness, and surface chemistry of the outer atomic layers, alloying elements in the melt, the gas environment of the particles when injected into the melt, stirring temperature, and holding the time in the melt. The discontinuously reinforcement phase composites are common due to availability, low cost, independence of mechanical properties from particulate orientation [20] and ease of production via a wide range of manufacturing routes [17–21].

Corondum (Al_2O_3), α is a very important hard ceramic due to its resistance to abrasion wear and corrosion, its high thermal stability and high electrical resistance but not least its availability and relatively moderate price [22]. WC is used in hard metals as in the form of single crystal. It is highly anisotropic [22]. Titanium carbide and titanium diborides are the most inert and the hardest of all the carbides and borides [23]. TiB_2 is a hard material with a high resistance to wear and high tensile strength at high temperatures. The high density combined with the compressive strength and the high modulus of elasticity leads to its use in shields elements. TiB_2 resists most reagents and it has an excellent wettability and stability in liquid metals.

Most of transition metal diborides have been considered to exhibit high mutual solubility. Complete solid solubility with a miscibility gap at lower temperatures has been shown for the TiB_2–CrB_2 system. Limited low-temperature boundary solubility and large homogeneity ranges at high temperatures have been observed for the TiB_2–WB_2, and CrB_2–WB_2 systems [24]. Some studies have been proceeded on boron carbide-based composites with transition metal diborides—in particular with TiB_2—have been extensively studied for cutting tools and wear parts [24].

TiB_2–W_2B_5 composite ceramics can be produced by reaction hot pressing [25]. The initial powders consist of B_2O_3, Al, which are then alloyed with WC and TiC. During sintering, the Al reacts with B_2O_3, and then the carbides react with B, thus promoting the formation of the desired transition metal borides. Above the eutectic temperature, boron and molten Al form, which promotes liquid phase sintering depending on the volume fraction. The reaction mechanism proceeds as follows: WC and TiC react with elemental boron forming borides such as WB_4, W_2B_5, and TiB_2. These reactions occur between 900 °C and 1,100 °C [25]. Ti will sometimes be added as an inoculant to the high chromium cast iron melts. The free Ti will immediately form small cubic particles of the TiC in the high C-melt. As the rest of the iron starts to solidify, these small particles act as nucleation sites for carbides and austenite. The uses of TiB_2 with WC guarantee this chemical potential for the reactions, and enhance the effectiveness of the TiB_2 [26]. In addition to the borides and carbides, the inoculants can also include alloy powders. For this investigation, FeAlTi additions have been considered. Fe has been shown to be beneficial for metallic and intermetallic binders in non-ferrous alloys [27]. Ti and Al additions are needed in order to avoid the formation of undesirable borides. The resulting ceramic powders exhibit a microstructure with grains of TiB_2, Al_2O_3 surrounded by metallic or intermetallic (Fe–TiAl) phase with a volume fraction of 20–30% in microstructure of particulates prior to injection in the molten alloy.

The wear resistant metal matrix composites (MMC) have been developed that independently allow the selection of hard particles, like carbides, borides, and nitrides, and a metal matrix. Generally, the two primary characteristics of wear resistant materials serve different purposes: the hard particulates impede wear by grooving or indenting mineral particles whereas the metal matrix provides sufficient toughness. Both properties depend on the amount, size, and distribution of the reinforcement as well as on the hardness and fracture toughness of both constituents and the bond between matrix and hard phases [1].

It is the objective of this work to produce ceramic particulates with TiB_2 phases, and then adding these particulates by inoculation into a molten 20Cr–3Mo–4C alloy to form spherical hard particulates. It is thought that the formation of M_7C_3 carbides having a spherical form in austenite matrix will produce a microstructure with good wear resistance and toughness.

Experimental procedure

The chemical compositions and physical characteristics of the FeTi, B_2O_3, and FeW particulates are given in Table 1, respectively.

Production of the sintered reinforcement

FeTi, B_2O_3, Al particles with a size of 40–60 μm were used for the production of the inoculant material containing TiB_2 and Al_2O_3 as the hard phases [28]. The objective was to obtain a particulate with hard phases which would have high toughness, hardness and a density similar to that of iron. For this reason FeTi–B_2O_3–Al were mixed in a stoichiometric ratio to obtain particulates containing the TiB_2 [28] phase. The exothermic dispersion process technology, developed by Martin Marietta [29], was used to produce the particulates. This process utilizes a mixture of powders of the ceramic particulate components (X and Y) and the third metallic component (A). Heating this mixture results exothermically interaction between X and Y components above the melting point of component A, but below that normally required to produce the ceramic phase XY. Through this reaction, fine hardening particles are formed in the solvent phase. With this process it is possible to obtain synthesized particulates containing 20–75 vol%

Table 1 The chemical compositions of the 20Cr–3Mo–4C alloy, FeTi B_2O_3, and FeW particulates

Cast alloy	Chemical composition (vol%)								
Elements	C	Mn	Si	Mo	Fe	Cr	S	P	Cu
Amount (wt%)	4.3	0.5	1.6	3.2	Bal.	26	0.03	0.03	0.04
Reinforcement particulates (purity, greater than 99%)									
Elements amount (wt%)	W	Ti	Si	%S	Fe	Al	B	C	%P
FeTi		75	0.5	0.03	Bal.	4.5		0.3	0.03
B_2O_3In 95 wt% purity, rest is H_2O									
FeW	80		0.5	0.05	Bal			0.5	0.04

reinforcement. The objective in this program was to obtain synthesized particulates containing the desired reinforcement phase: homogenously distributed TiB_2 in the particulates.

Literature shows that in some studies where Ti, B, and Al are used, the particulates resulting in the formation of TiB reinforcing particles with a size of 1–10 μm [30]. In some studies the reaction strengthening of the Ti/Al composites by isothermal heat treatment indicated that isothermal heat treatment at 853 K results in the reaction between Ti and Al giving Al_3Ti phases. The formation of Al_3Ti leads to increases in strength and modulus of the composites [31].

For the Ti–Al–B system, the reactions of reinforcements can form during the process:

$$\mathrm{Al(s)} = \mathrm{Al(l)} \quad (1)$$

$$\mathrm{Ti(s)} + 3\mathrm{Al(l)} = \mathrm{Al_3Ti(s)} \quad (2)$$

$$\mathrm{Ti} + \mathrm{B_2O_3} + \mathrm{Al} = \mathrm{TiB_2} + \mathrm{Al_2O_3} \quad (3)$$

$$\mathrm{TiB_2} + \mathrm{Ti} = 2\mathrm{TiB} \quad (4)$$

The reaction 3 proceeds continuously during sintering.

The sintered compacts then ground an average size of 40 μm, and these ground particulates were used for inoculation into the melt.

The average carbide size and volume fraction were determined by quantitative metallography using a digital image analyzer leica Q550.

Production of the inoculated high Cr white cast iron

When the temperature of the melt was at least 50 C-deg above the pouring temperature, a preheated stirrer was introduced in the melt. Agitation of the melt was started at the desired 1,000 rpm as 3 min and the inoculant particles of 40 μm were introduced in the vortex in the ratio of 5 wt%. The stirring was continued to prepare homogenous slurry. The slurry was cast into a permanent steel mould of size 25 × 30 × 300 mm, by removing the graphite stopper from the bottom of the crucible. The slurry was pored into preheated die cavity (475 K). The preheated ram attached to hydraulic press, which was used to maintain 50 MPa pressure during alloy infiltration into composite. This pressure was maintained for 40 s.

Three groups of samples were produced (Table 2). The first group was produced by the inoculation of particulates obtained from Al–FeTi–B_2O_3 particles. The second group was produced by the inoculation of sintered particulates obtained from the mixture of Al–FeTi–B_2O_3–FeW particles. The third group was obtained by homogenization heat treatment of the second group. Homogenization heat treatment used in this investigation involved annealing at 1,200 °C for periods of 0.5, 1, 3, and 6 h, followed by air-cooling.

Characterization and evaluation

To examine the effect of the particulates on the composite microstructure, specimens were characterized X-ray Diffraction (XRD), and by both optical and scanning electron microscopy (SEM). For optical metallographic evaluation, the specimens were polished and subsequently etched in a solution containing 5 g $FeCl_3$, 30 mL

Table 2 The heat treatment of the samples

Sample	Composition	Heat treatment
S1	20Cr–3Mo–4C	–
S2	20Cr–3Mo–4C–1B–0.5Ti	–
S3	20Cr–3Mo–4C–1B–0.5Ti–2.5W	–
S4	20Cr–3Mo–4C–1B–0.5Ti–2.5W	30 min, 1,200 °C
S5	20Cr–3Mo–4C–1B–0.5Ti–2.5W	1 h, 1,200 °C
S6	20Cr–3Mo–4C–1B–0.5Ti–2.5W	3 h, 1,200 °C
S7	20Cr–3Mo–4C–1B–0.5Ti–2.5W	6 h, 1,200 °C

HCl, and 100 mL distilled water. Scanning electron microscopy characterization was performed on (as-polished?) specimens using a (JEOL 5600 SEM + ISIS EDS) scanning electron microscope operated at 20 kV. This instrument was also contained an energy dispersive X-ray spectrometer and analysis system for microanalysis.

The abrasive wear tests were performed using a pin-on-disc type apparatus. Before the wear tests, each specimen was ground to grade 1,200 abrasive paper. Abrasive wear tests were carried out under the load of 20, 80, and 140 N on a grade 80 abrasive paper attached to the grinding disk, which rotated at 320 rev min^{-1}. A fixed track diameter of 160 mm was used in all tests, and the duration of the abrasion test was 60 s. Each test was performed with a fresh abrasive paper, and, for each test condition, a minimum of three runs were performed. Wear rates were obtained by measuring the masses of the samples before and after wear tests.

Microstructure

The microstructure of 20Cr–3Mo–4C white cast iron

The microstructure of the white cast iron varies significantly as a function of chemical composition. The aim of this investigation was to inoculate the 20Cr–3Mo–4C white cast iron to produce a microstructure containing spherical hard phases for high wear resistance with high toughness. In general, the samples containing 20 wt% Cr are composed of an austenitic matrix and M_7C_3 carbides, with a layer of austenite surrounding the carbides. The microstructure also contains proeutectic austenite dendrites and eutectic cells composed of M_7C_3 carbides and an austenite phase. The microstructure of the sample S_1 (20Cr–3Mo–4C) is presented in Fig. 1.

In the microstructure of the 20Cr–3Mo–4C white cast iron (Fig. 1), large proeutectic M_7C_3 carbides with non-uniform size distribution are dominant, and the eutectic cells (γ and M_7C_3) formed throughout the rest of the microstructure. The carbides in the sample S_1 have blade-type morphology, although there are some rod-like carbides. Furthermore, the blade-like carbides are generally appeared around the large proeutectic M_7C_3 carbides. The core of the M_7C_3 carbides is split before the peritectic reaction temperature is reached. Therefore the proetutectic M_7C_3 carbides may not react with the liquid to form the core and rim structure. For this reason, it was thought that the addition of the particulates prior to casting would enhance nucleation of proeutectic M_7C_3 carbides, as well as the eutectic formation from austenite and M_7C_3 from the liquid phase.

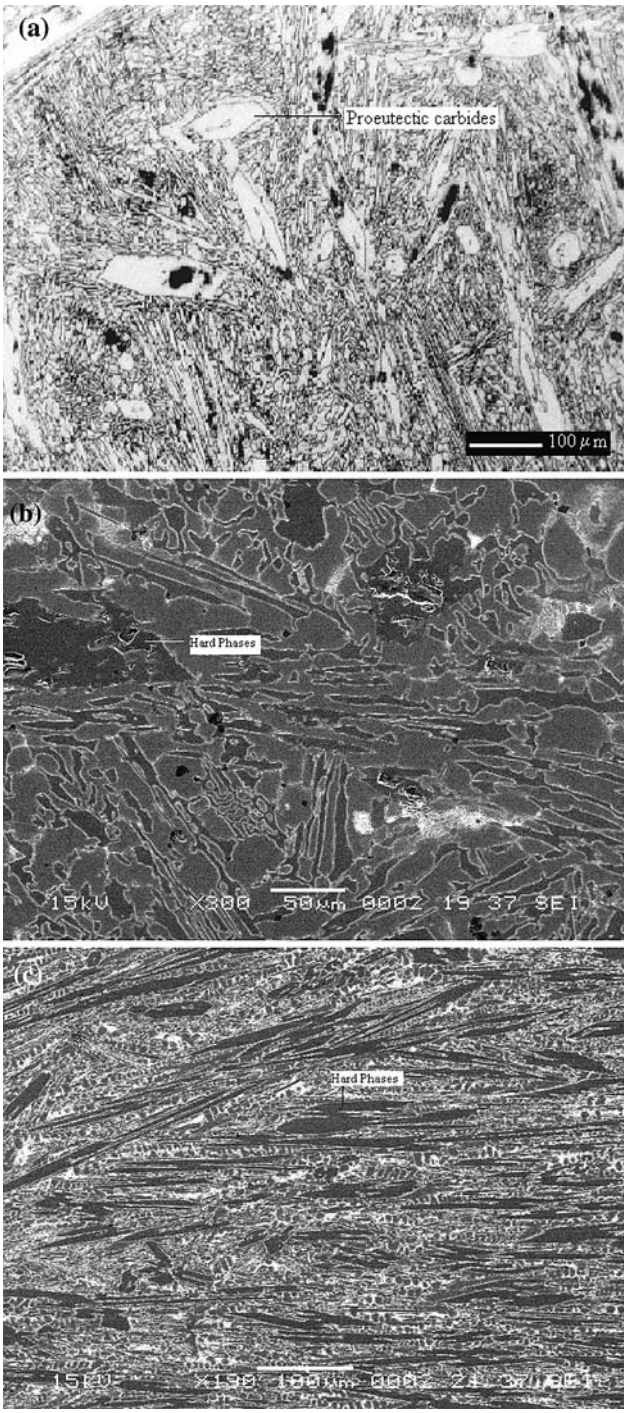

Fig. 1 (**a**) Optical micrograph of sample S_1 (×200), (**b**) SEM micrograph of sample S_1 (×200), and (**c**) SEM micrograph of sample S_1 (×200)

The microstructure of inoculants particulates

Depending on the amount of additives the other ceramic phases Al_2O_3, Al_3Ti, TiB phases form. The X-ray diffraction data (see Fig. 2) revealed that the Al_3Ti phase

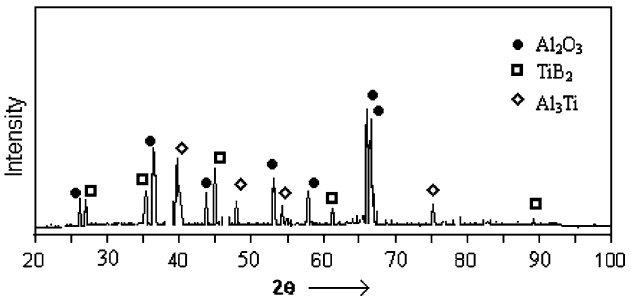

Fig. 2 X-ray diffraction of reinforced particulates

formed. This phase is known as an intermediate phase having low density, high melting point, high hardness, and high young modulus. On the other hand, it has a tetragonal structure and it is very brittle [29]. Although this phase is not preferable for structural materials, it can be beneficial for wear resistance applications if it is dispersed throughout the matrix. Increasing the concentration of B in the particulate decreases the amount of the Al_3Ti and increases the proportion of TiB_2 with the reaction of 3. The Fig. 2 shows the XRD results of the (TiB_2 + Al_3Ti + Al_2O_3)/Al produced from the Ti–Al–B. The XRD results confirm the presence of TiB_2, Al_2O_3, and Al_3Ti phases in the sintered compacts.

For the second group inoculants FeW particulates was added to the mixture. The purpose of this addition is that; it is known that carbides and borides of W decompose above 1,600 °C in the presence of TiB_2, and a solid solution of (Ti, W) B_2 forms with increasing solubility of W by increasing temperature [32].

The microstructure of (FeTi–B_2O_3–Al) inoculated 20Cr–3Mo–4C white cast iron

The metallographic evaluation of these samples show that the hard particulates were not homogeneously dispersed in the matrix, possibly due to their density difference between externally added particulates and molten matrix, but rather that the particulates became heterogeneous nucleation sites for the formation of carbides. The carbide morphology in high chromium white cast iron morphology consists of rod- and blade-like structures characterized by a growth direction along the axis of the rod or blade. The growth of the rod- and blade-like structures is confirmed within an eutectic call for hypoeutectic and eutectic irons. On the other hand in hypereutectic irons the carbides can be extremely thick and long. The length of a hypereutectic rod is only limited by the growth of adjacent hypereutectic rods within the melt [33]. Depending on the microstructural shape, EDS analysis, and microhardness of the carbides it is thought that hypoeutectic carbides were formed in the

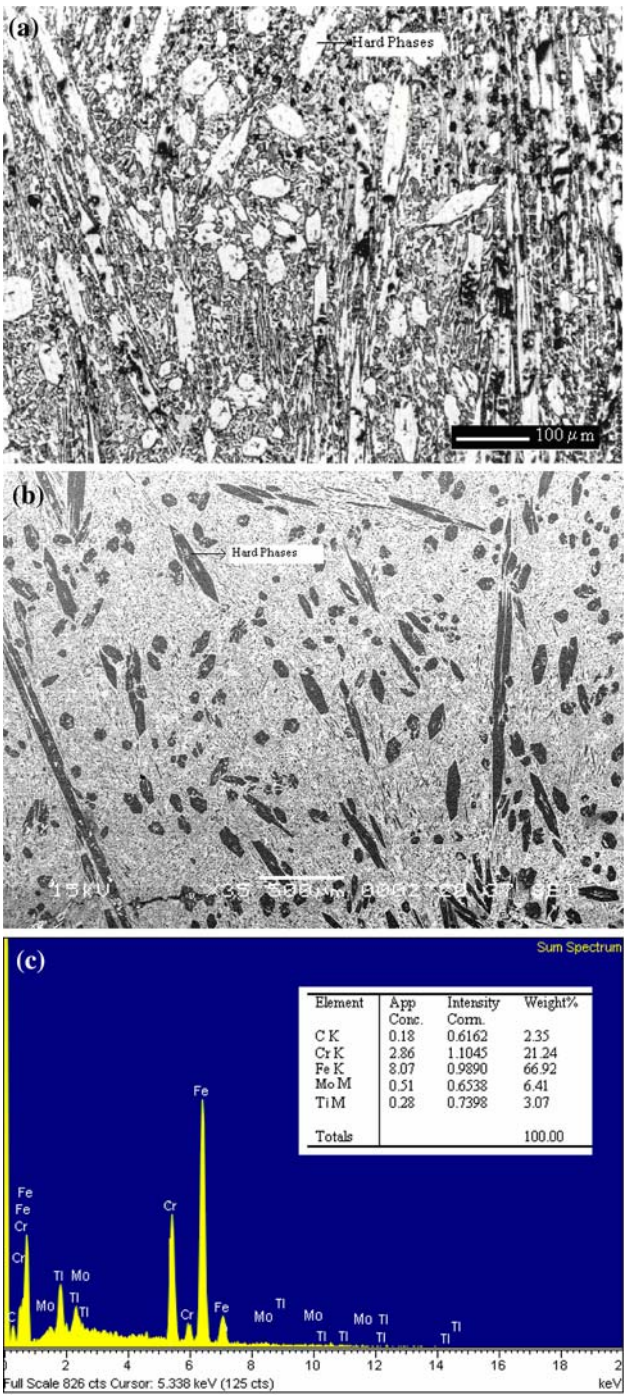

Fig. 3 (**a**) Optical micrographs sample S_2 (×500), (**b**) SEM micrographs of sample S_2, (**c**) EDS analysis of S_3

structure during solidification (see Fig. 3a–b). The EDS analysis of the carbides is given in Fig. 3c. The obtained microstructure indicates that this technique does not yield a desired structure, possibly due to the density difference between Ti and Fe, and affinity of Ti to oxygen (and propensity to form TiO_2). These results revealed that it had not been possible aim to form TiB_2-containing particulates that

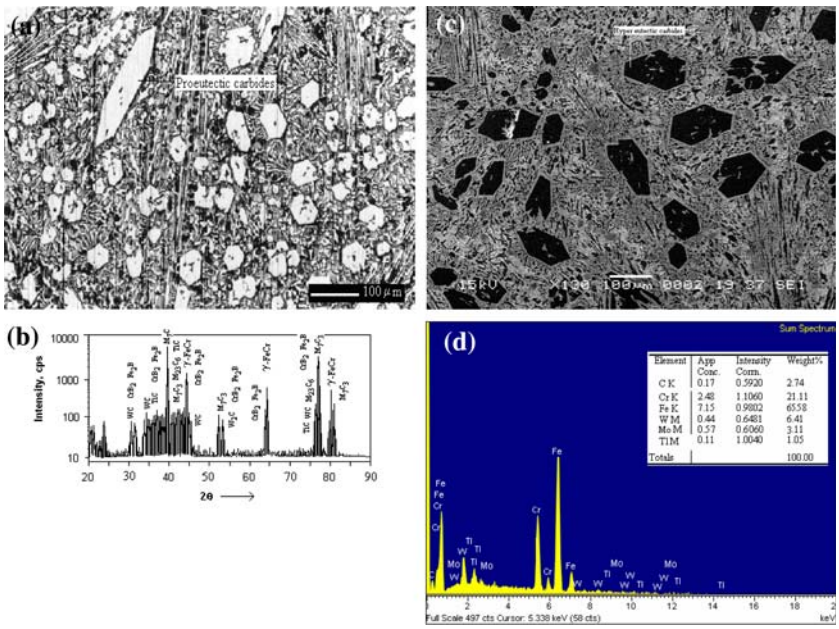

Fig. 4 (**a**) Optical micograph of S_3, (**b**) X-ray diffraction of the sample, (**c**) SEM micograph of sample S_3, (**d**) EDS analysis of S_3

were stable at casting temperatures, for this reason this approach needs to be improved. Hence, FeW was added to the inoculation particulate for more appropriate particulate production.

The microstructure of (FeTi–FeW–B_2O_3–Al) inoculated 20Cr–3Mo–4C white cast iron

FeTi–B_2O_3–Al–FeW particulates were mixed and sintered as inoculants for the second reinforcement group. The as-cast samples were metallographically evaluated. The resultant microstructures suggested that these added particulates were effective nucleation sites for the eutectic phase and primary carbides that form during solidification in the hypereutectic region. The microstructure of the sample shown in Fig. 4a, c contains proeutectoid white cast iron. Proeutectic carbides containing significant amounts of W were observed (Fig. 4b, d). It seen from microstructure that the particulates added to the structures during casting have acted as nucleation point during formation of proeutectoid carbides. In addition to the carbides, also an inter-dendritic phase Fig. 5a–b similar to the ledeburite phase was seen.

The microstructure of (FeTi–FeW–B_2O_3–Al)-inoculated 20Cr–3Mo–4C white cast iron after 1,200 °C homogenization treatment

The homogenization heat treatment was used to obtain a more homogenous distribution of carbides in the microstructure. The microstructure of the sample heat treated for 0.5 h at 1,200 °C is presented in Fig. 6a. Semi-quantitative

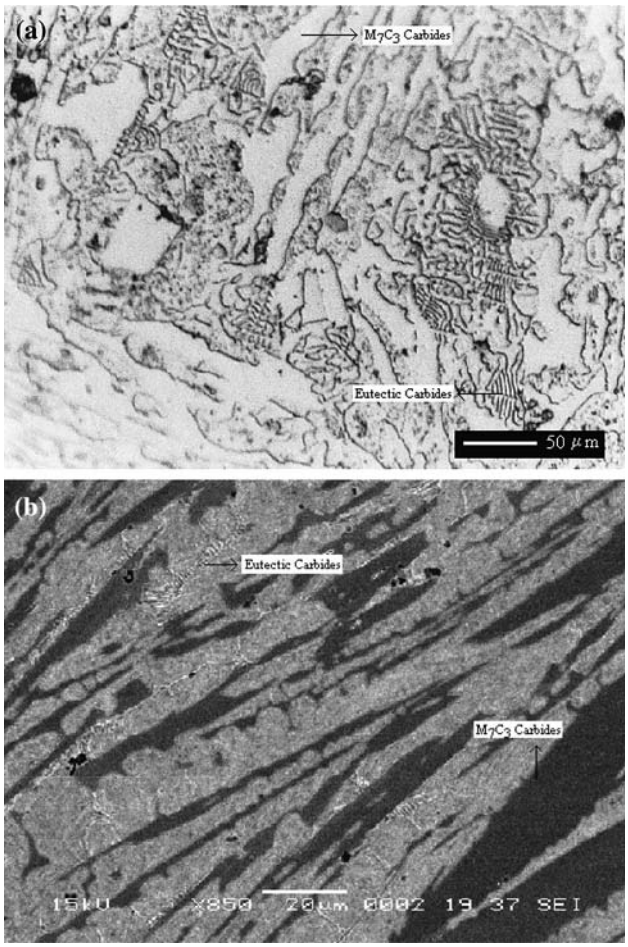

Fig. 5 (**a**) Optical micrographs sample S3 (×750), SEM micrograph of sample S3

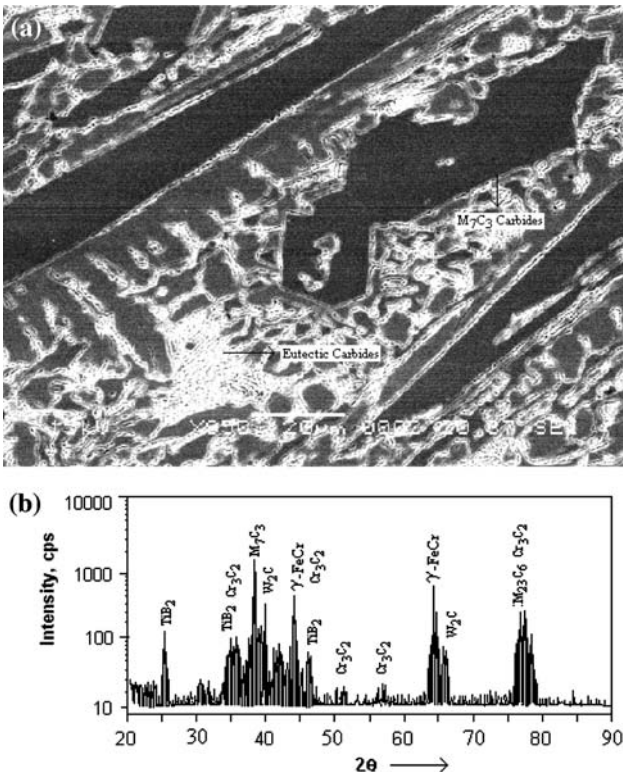

Fig. 6 (**a**) SEM micrograph of sample S_4, (**b**) X-ray diffraction of the sample

EDS analysis of the coarse phases observed Fig. 6 is listed in Table 3. Three phases were observed in the microstructure. Based on the microhardness and the EDS analysis, gray region was identified as the matrix, black regions were consistent with M_7C_3 carbides, and the white region was the W-enriched (~23 wt% W) eutectic phase (Fig. 6b).

The homogenization period at 1,200 °C results in a refinement of the hard phases in the microstructure (Fig. 6b). The proeutectoid particulates were distributed in the microstructure more homogeneously as the homogenization time increased. In addition, the homogenization treatment caused changes in the surface hardness and microstructure, as listed in Table 4. It was observed that the microhardness of some carbides was greater than 3,000 HV. In addition depending on the EDS analysis we have seen that these hard phases are consisting of W, Mo, T, C, B elements. The second type hard phases, which were distributed more readily have a micro hardness over 2,000 HV. It is assumed that this carbides should be M_2C carbides having especially W, Mo, Ti, C, and B elements. The third hard phase was obtained as a phase having 1,700 HV micro hardness, and this phase is assumed to be as M_7C_3.

Table 3 EDS analysis of the S_4

Elements	White region (eutectic) phase (wt%)	Gray region (matrix) (wt%)	Black region (M_7C_3) (wt%)
Cr	9	8	43
Fe	62	89	38
W	23		7
Ti	2		2
Mo	<1	–	5

The microstructure of the sample S_5 is shown in Fig. 7. Qualitative EDS analysis results are listed in Table 5. The microstructure of the sample S_6 is given in Fig. 8. It was noted that the carbides have been refined considerably by increasing the homogenization time from 1 h to 3 h. The microstructures of the S_6 show that the primary carbides have partially dissolved and spheroidized particulates were obtained. MC and M_2C particulates were also observed in the microstructure. The homogenization heat treatment time was increased to 6 h for sample S_7. Homogenously distributed particulate were seen in the microstructure of S_7. The microstructure obtained for the sample S_7 is given in Fig. 9. The microstructure of the sample S_7 having a heat treatment of 6 h at 1,200 °C have shown that the size of primary (M_7C_3) and secondary carbides (M_2C and MC) are approximately the same, and the hard particulates have decreased their sizes to the 40 μm. It was seen that W, Ti, and Cr are present in the structure of the carbides.

The volume fraction of carbides in the samples obtained by image analysis, and the results listed in Table 4. The literature on the white cast iron show that there is a relation between carbide volume ratio and chemical analysis as CVR = 14C + 0.43Cr – 0.22 [13, 34]. But, in this investigation the application of this equation is not reasonable. The chemical concentration and the amount of carbides were changed due to the externally added hard particulates. In other words, the sintered inoculant particulates are produced from FeTi–FeB–Al–FeW particulates. It is possible that during solidification the inoculants altered the solidification gradient. In Table 4 the hardness of the phases are given for all samples. It is seen from the Table 4 that the maximum hard phase ratio was detected for sample S_7. Depending on the microhardness of hard phases and the XRD results it was observed that the carbide phase in all these regions is primarily M_7C_3 type. Hardness of the hard particulates in sample S_3 have a high hardness up to 3,300 HV. The application of heat treatments shows that the hardness of the hard phases has decreased and the carbide volume ratio increased due to decomposition of the hard phases. A similar result is seen for ledeburite phases.

The abrasive wear rate of the inoculants reinforced 20Cr–3Mo–4C white cast iron

The relationships between wear rate and the load are given in Fig. 10 for particulate reinforced and heat treated samples.

Table 4 The microstructure and surface hardness values of samples

Sample num.	Primary carbide hardness HV	Ledeburite phase hardness HV	Hard phase ratio vol%	Matrix HV	Surface hardness HRC
S_1	1,550	–	38.4	670	53
S_2	2,000–2,400		42	800–850	57
S_3	2,700–3,300	1,600–1,700	49.6	800–1,000	63
S_4	2,600–3,000	1,500–1,700	51	800–1,000	63
S_5	2,500–2,800	1,500–1,700	52.1	800–1,000	64
S_6	2,300–2,400	1,300–1,450	62.2	800–1,000	65
S_7	1,900–2,000	1,100	58.6	800–1,000	67

The lowest wear rate was seen from the sample of S_3. It is thought that, in sample S_3 the particulates reinforced the structure by their both particle shape and particle strength because the tribological behavior of a composite depends on the microstructural properties of the material and also on the type of loading-contact situation [35]. It is clear that the particulate reinforcements caused an important decrease in wear rate of the composites during abrasive wear. On the other hand, the abrasive tests with particulate reinforcement showed that the increase of particulate hardness in the matrix decreased wear rate. However, the homogenization treatment decreased the wear resistance of the samples (Fig. 10). It is speculated that the decrease of wear rate is strongly dependent on the decrease of the size of carbides and matrix, the microhardness of carbides and due to the distribution of the particulates in the matrix [36–37]. Sin et al. [25] indicated that the size of abrasive grit had a direct influence on the associated wear mechanism. Depending on the size of the abrasive grit, abrasive particle would either plastically deform the surface or cut it. The size ratio between reinforcement and grit is therefore extremely important. As the wear particles became duller or the particle size decreased, the wear mechanism exhibited a transition from cutting to delamination wear [38]. Moreover, there is a critical particulate size [39]. The wear rate increases with the applied load up to a critical particulate size [8]. Above the critical values, the wear rate was largely independent to the particulate size and the load. In addition, the hardness differences between the particulate and the matrix material influences this critical value [8]. For this reason, the particulates having different hardness, toughness, and structures were used as hybrid at sample S_3 to increase the critical load at where wear changes from microcutting to microcracking.

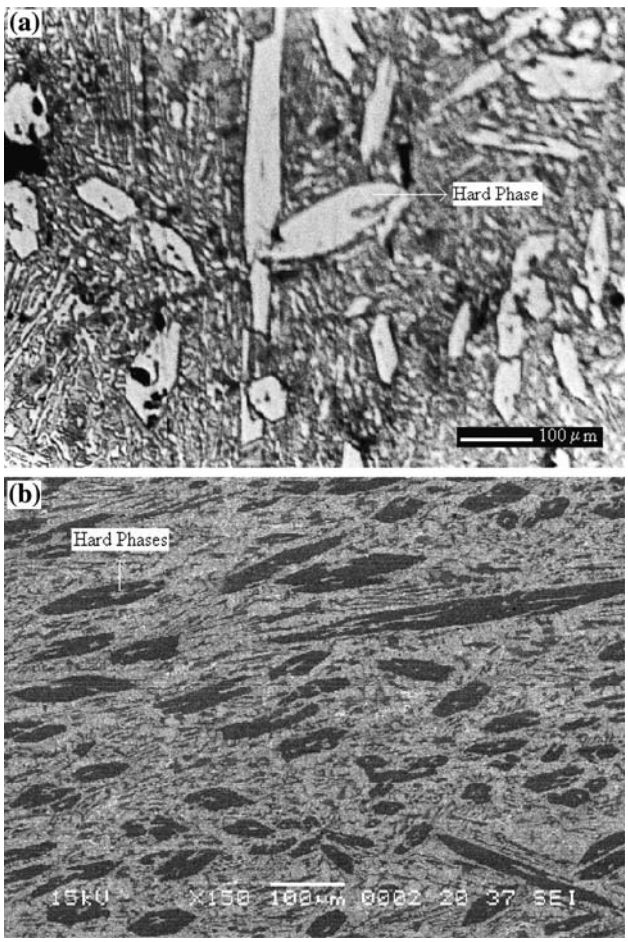

Fig. 7 The microstructure of sample S_5

The wear resistance of the composites exhibited a strong relationship with the homogenization treatment conditions, and is presented in Fig. 11. Moore and Doutwaite suggested that, during abrasive wear, the extent of the plastically strained region below an abraded surface depended on the abrasive grit size and the applied load [9]. The overall depth of the plastic deformation was linearly related to the applied load and the grit dimensions. Figure 11a shows the relationship between carbide vol% and wear

Table 5 EDS analysis of phases for sample S_5

Phases	Composition (wt%)				
	Cr	Fe	Ti	W	Mo
Primary M_7C_3	68	26	1	–	5
Matrix	10	90	–		–
Ledeburite	33	61	–	6	–
Secondary hard phases	15	54	2	27	2

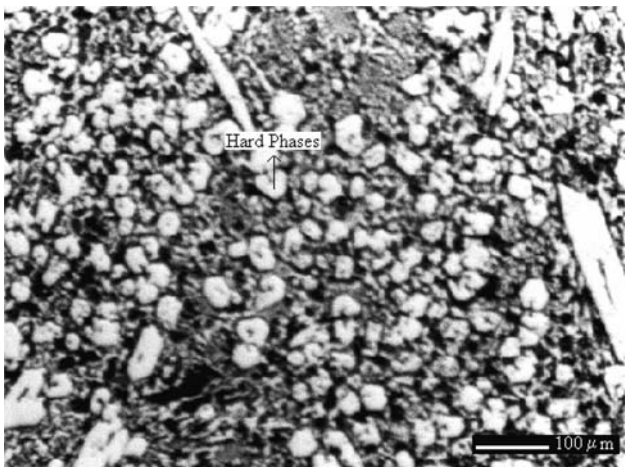

Fig. 8 Optical micrographs of sample S_6 (×500)

rate, and Fig. 11b illustrates the relationship between primary carbide hardness and wear rate. It can be seen that the carbide vol% and primary carbide hardness have major effects on the wear rate. The increase in the homogenization treatment time to 6 h produced a microstructure in which carbides are spheroidized, but the wear rate of this structure is lower than the sample S_3.

Conclusion

Addition of hard inoculants as mixture of Ti–B–W to a high Cr white cast iron has resulted in a structure containing hard carbide particulates distributed homogeneously in microstructure.

1. The microhardness of the hard particulates exhibited hardness up to 3,300 HV.

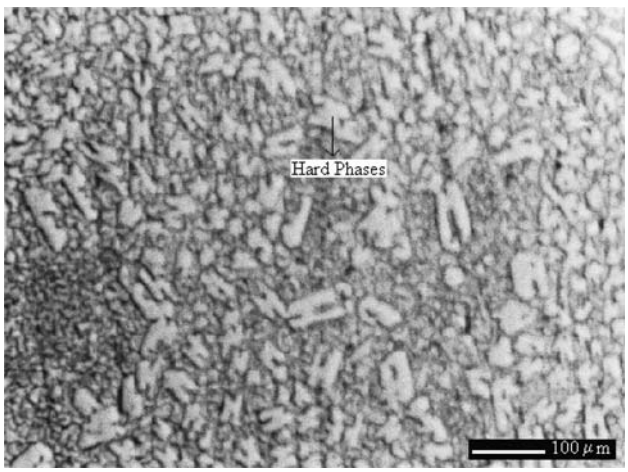

Fig. 9 Optical micrograph of sample S_7 (×500)

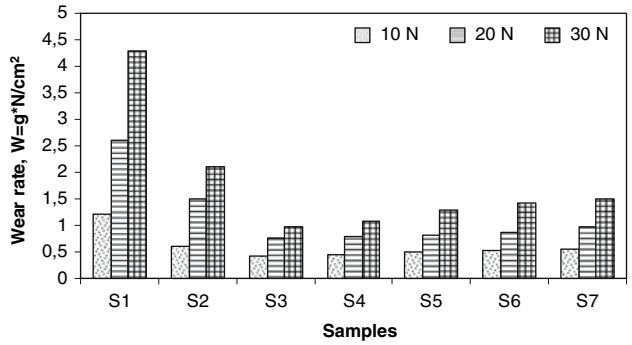

Fig. 10 The wear rate versus load for the samples

2. The microstructures of the samples are characterized by an austenitic matrix and M_7C_3 carbides, with a layer of austenite surrounding the carbides.
3. The application of an homogenization heat treatment to the as-cast inoculated alloy resulted in an significant refinement of the microstructure. Increasing the homogenization time resulted in the decomposition of coarse WC particulates, and the formation of ledeburite phases.
4. The lowest wear rate was obtained for sample S_3.
5. The sample S_2 having inoculants without W did not gave homogeneously distributed carbides, and its wear rate is higher than sample S_3.

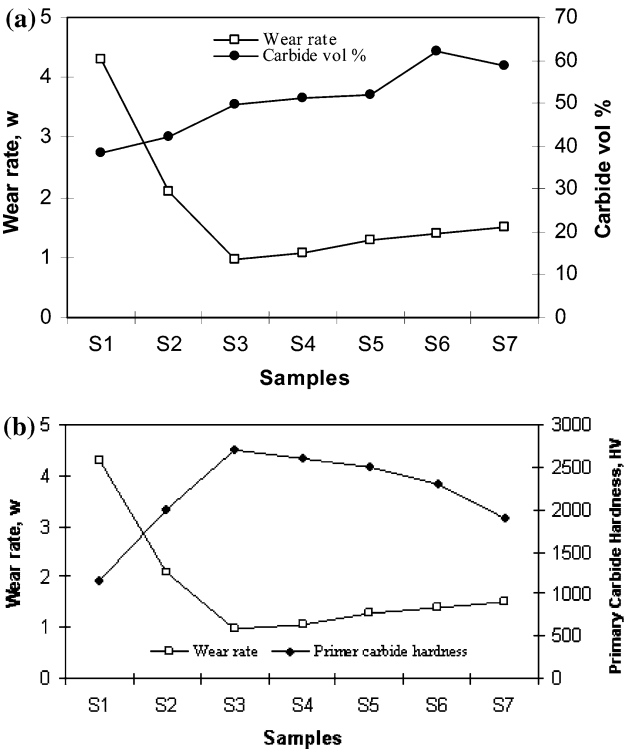

Fig. 11 The relationship between (**a**) Carbide vol%—Wear rate (20 N load), (**b**) Primary carbide hardness—Wear rate (20 N load)

References

1. Kulkarni KM, Anand V (1984) Metals handbook, 9th edn. ASM, Metals Park, OH 7:823
2. Kinzel AB, Crafts W (1937) The alloys of iron and chromium. Mcgraw-Hill, New York, NY, I:25
3. Kinzel AB, Franks R (1937) The alloys of iron and chromium. Mcgraw-Hill, New York, NY, II:173
4. Gundlach RB, Parks JL (1978) Wear 46:97
5. Maratray F (1971) AFS Trans 79:121
6. Parks JL (1978) AFS Trans 86:93
7. Zum Gahr KH, Doane DV (1980) Metal Trans A 11A:613
8. Zum Gahr KH, Eldis GT (1980) Wear 64:175
9. Fulcher JK, Kosel TH, Fiore NF (1983) Wear 84:313
10. Gundlach RB, Parks JL (1978) Wear 46:97
11. Junyi S, Yuding J (1987) In: Ludema KC (ed) Wear of materials. ASME, New York, NY, pp 661–671
12. Tabrett CP, Sare IR, Ghomashci MR (1996) Int Mater Rev 41:59
13. Ray S, Rohatgi PK (1972) Ind Patnet 30A:124
14. Badia M, Rohatgi PK (1969) Trans Am Foundrymen's Soc 79:402
15. Mehrabian R, Flemings MC (1976) New trends in materials processing. ASM, Metals Park, 98
16. Ghosh K, Ray S, Rohatgi PK (1984) Trans Jpn Inst Met 25:440
17. Elanny F, Froyen L, Deruyttere A (1987) J Mater Sci 22:1. DOI: 10.1007/BF01160545
18. Mortnesen A, Cornie JA, Flemings MC (1988) J Metals 40:12
19. Mortnesen A, Cornie JA (1987) Met Trans 18A:1160
20. Mcdanels L (1985) Metal Trans 16A:1105
21. Hosking M, Pportillo FF, Wunderlin R, Mehrabian R (1982) J Mater Sci 17:477. DOI: 10.1007/BF00591483
22. Reidel R (2000) Handbook of ceramic hard materials. Willey-vch, Verlag GmbHD-69469 Weinheim, Germany, p 648
23. Laird G, Gundlach R, Rohrig K (2000) Abrasion-resistant cast iron handbook. American Foundry Society, Illinois, p 72
24. Nishiyama K, Mitra I, Momozawa N, Watanable T, Abe M, Telle RJ (1997) Jpn Res Inst Mater Technol 15:292
25. Telle R, Petzow G (1988) Mater Sci Eng A105/106:97
26. Sanchez JM, Azcona I, Castro F (2000) Bol Soc Esp Ceram Vidr 39(3):251
27. Vergara V, Lopez M, Benavente R, Camurri C, Cartes B (1999) In: Proceedings of copper 99-international conference, 1:303
28. Tjong SC, Wang GS, Mai YW (2003) Mater Sci Eng A 358:99
29. Rack HJ, Kumar P, Vedula K, Ritter A (eds) (1988) In: Processing of properties of powder metallurgy composites. The Metallurgical Society, PA, p 155
30. Yilmaz O (2001) Mater Sci Technol 17:1285
31. Ma ZY, Bi J, Lu YX, Shen HW, Gao YX (1993) Compost Interface 1:287
32. Raganath S, Vijayakumar M, Subrahmayam J (1992) Mater Sci Eng A 149:253
33. Powel GLF, Laird G II (1992) J Mater Sci 27:29. DOI: 10.1007/BF00553833
34. Riedel R (2000) Handbook of ceramic hard materials. Wiley-vch Verlag Gmbh, Weinheim
35. Zum Gahr KH, Eldis GT (1980) Wear 64:175
36. Kinzel AB, Franks R (1937) The alloys of iron and chromium. Mcgraw-Hill, New York, NY, II:173
37. Gundlach RB, Parks JL (1978) Wear 46:97
38. Zum Gahr KH (1979) Met Prog 116:46
39. Powel GLF, Carlson RA, Randle V (1994) J Mater Sci 29:4889. DOI: 10.1007/BF00356539